Summary of research results

1) **Determine the role of the type 2 iodothyronine deiodinase (D2) production of tanycytes in the regulation of the hypothalamic-pituitary-thyroid axis, in addition, we will elucidate the relative involvement of the α and β tanycytes in this neuroendocrine regulatory mechanism**

As we described in the interim reports, as a first attempt, we generated nestinCreERT2-DIO2FLX/FLX and treated these animals with tamoxifen to knock our D2 from tanycytes. We could not decrease the D2 activity in the mediobasal hypothalamus (MBH) where D2 is produced by tanycytes, but we observed a marked decrease of D2 activity in the cortex of these animals. As nestin should not express in the cortex of adult mice, we crossed nestinCreERT2 mice with tdTomato expressing indicator mice. Adult, double transgenic mice were treated with vehicle or with tamoxifen and the tdTomato expression was studied. While tamoxifen induced strong tdTomato expression in tanycytes, a tamoxifen treatment independent tdTomato expression was observed in neurons and astrocytes of many brain regions including the cortex demonstrating that the nestinCreERT2 mice are not sufficiently specific despite of the fact that this mouse model is widely used. To solve this problem, RaxCreERT2 mice were imported. By crossing these mice with tdTomato expressing indicator mice, tdTomato expression was observed only in tamoxifen treated animals and only in tanycytes demonstrating the specificity of the model. In RaxCreERT2-DIO2FLX/FLX mice, however, we could not knock down the D2 expression of tanycytes despite the fact that we tried several different method (intraperitoneal administration, gastric gavage, tamoxifen containing diet and combination of tamoxifen containing diet with intraperitoneal administration) at different age of mice (adult, 10 day old, 4 day old). All of these approaches were sufficient to induce recombination when the RaxCreERT2 mice were crossed with tdTomato indicator mice suggesting that the DIO2 gene may have special chromatin structure in tanycytes that prevents the Cre induced recombination. We also made attempt to knock out the DIO2 gene by Crisper Cas9 technology. To optimize the method, we tried two different guide RNAs in cell culture, but none of these yielded positive results. Due to these unexpected difficulties, we could not accomplish the aim of the first specific aim. However, we currently import floxed D3 overexpressing mice from Prof Graham Williams (Imperial College London, UK). With the help of these mice, we would like to overexpress the thyroid hormone inactivating enzyme, D3, specifically in tanycytes to degrade all D2 activated thyroid hormones within the tanycytes. Our hypothesis is that we should achieve similar results with tanycytic D3 overexpression than what we could achieve with D2 knock down and this way, we will be able to determine the importance of the thyroid hormone activation of tanycytes in the regulation of the HPT axis.

2) **Elucidate the role of the endocannabinoid system in the regulation of the secretory activity of hypophysiotropic TRH neurons by tanycytes**

To determine whether the hypophysiotropic TRH neurons express the CB1 receptor, double-labeling *in situ* hybridization was performed. CB1 mRNA was observed in the majority of neurons in the hypothalamic paraventricular nucleus (PVN) where the perikaryon of the hypophysiotropic TRH neurons reside; however, the intensity of the hybridization signal was much lower than that observed in cortical or hippocampal areas. Analyses of the double-labeled sections showed that silver grains denoting CB1 mRNA were observed above 73.4±1.5% of the TRH neurons in the PVN (Fig. 1A). In addition, double-labeling immunofluorescence using a novel rat anti mouse proTRH antibody generated in our laboratory showed that punctuate CB1-immunoreactive signal was present in the majority of TRH-IR axon varicosities in the external

zone of the ME suggesting that the hypophysiotropic TRH axons are sensitive to endocannabinoid signaling (Fig. 1B).

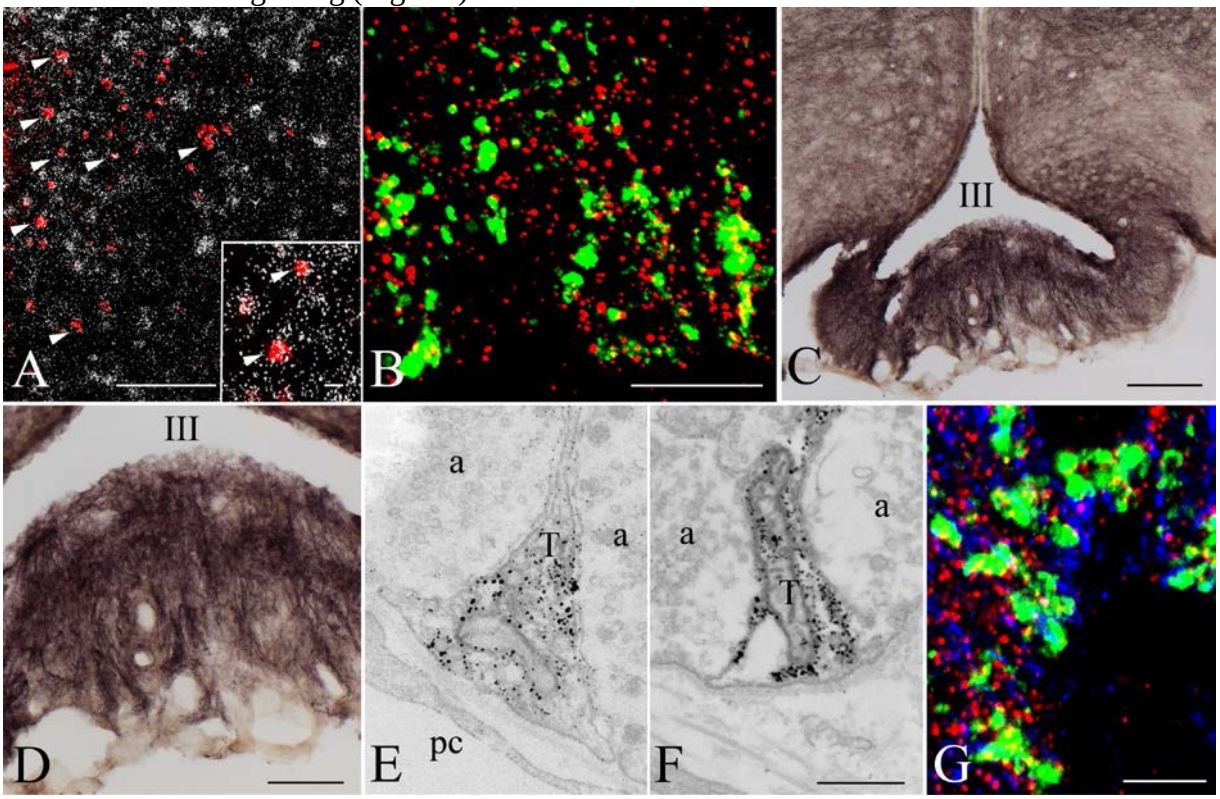

Figure 1. *Elements of the endocannabinoid system are present in the hypophysiotropic TRH neurons and in the tanycytes in the external zone of the ME.*
(A) Double-labeling in situ hybridization demonstrates that the majority of TRH neurons (red) in the PVN express CB1 mRNA labeled by the presence of silver grains. Arrowheads point to double-labeled neurons expressing both TRH and CB1 mRNAs. Inset illustrates double-labeled neurons at higher magnification (arrowheads). (B) Double-labeling immunocytochemistry demonstrates the presence of CB1-immunoreactivity (red dots) in TRH-IR hypophysiotropic axon varicosities (green) in the external zone of the ME. The CB1-immunoreactivity within the TRH axons appear yellow due to the color mixing. (C) High level of DAGLα-immunoreactivity is present in tanycyte cell bodies lining the floor of the third ventricle and the wall of the lateral evaginations. Dense DAGLα-IR fiber network is also present in the median eminence. (D) Higher magnification image illustrates that the DAGLα-IR fibers run perpendicular to the surface of the median eminence. (E, F) Ultrastructural images demonstrate that the DAGLα-immunoreactivity (labeled by silver grains) is present in tanycyte end feet processes terminating around portal capillaries. (G) The CB1-containing (red) TRH-IR (green) axon varicosities are closely associated to DAGLα-IR (blue) tanycyte processes. Scale bars = 100 µm on (A) and (C), 10 µm on inset and (B), 50 µm on (D), 0.5 µm on (F) that corresponds to (E) and (F), 5 µm on (G).
Abbreviations: III = third ventricle, a = axon varicosity, pc = portal capillary, T = tanycyte end feet.

To determine the cell type that releases endocannabinoids in the ME, the localization of diacylglycerol lipase α (DAGLα), the synthesizing enzyme of the endocannabinoid, 2-arachinodonoylglycerol (2-AG) was studied. At the light microscopic level, DAGLα-immunoreactivity was observed in tanycyte cell bodies lining the floor (β2 tanycytes) and the lateral evagination (β1 tanycytes) of the third ventricle (Fig. 1C). In addition, DAGLα-immunoreactivity was also observed in processes running towards the capillary plexus of the

external zone of the ME (Fig. 1D), reminiscent of the distribution of the β-tanycyte basal processes.
Immuno-electron microscopy demonstrated DAGLα-immunoreactivity to be present in tanycyte cell bodies and processes in the ME. In the external zone of the ME, DAGLα-IR end-feet processes of ß2 tanycytes were closely associated with axon terminals of hypophysiotropic neurons (Fig. 1E, F). Triple-labeling immunofluorescence demonstrated that axon terminals-containing both TRH-immunoreactivity and punctate immunofluorescence labeling the CB1-immunoreactivity are closely associated to DAGLα-IR tanycyte processes (Fig. 1G).

To determine whether endocannabinoids affect basal TRH release, ME explants were treated with the CB1 antagonist, AM251, or CB1 agonist, WIN55,212-2, in the presence of a TRH degreading enzyme (TRH-DE) inhibitor. AM251 stimulated TRH release causing an approximately 2-fold increase in the TRH concentration of the ME explant supernatant (Fig. 2A). The CB1 agonist, however, had no effect (Fig. 2A). To test the hypothesis that the exogenous CB1 agonist was ineffective because of saturation of CB1 by its endogenous ligand, the effect of WIN55,212-2 was tested in the presence of the DAGLα inhibitor, tetrahydrolipstatin (THL). Treatment of the explants with THL caused an increase in TRH release, while the CB1 agonist decreased THL-induced TRH release (Fig. 2B). These data demonstrate that endocannabinoids inhibit TRH release in the ME and there is a tonic, endocannabinoid-induced inhibition of TRH release in the ME explants.

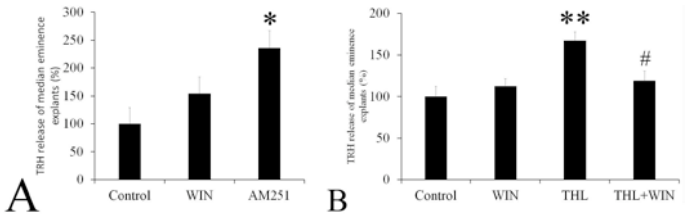

Figure 2. *Effects of pharmacological manipulation of the endocannabinoid system on TRH release from median eminence explants.*
*(A) TRH recovered from median eminence explants incubated in ACSF containing the TRH-DE inhibitor, P-TRH (200 nM), was measured by RIA. While WIN 55,212-2 (1µM) had no effect on the TRH release of from the median eminence explants, AM251 (1µM) induced a two-fold increase of TRH release. (B) To determine whether the absence of CB1 agonist effect is due to saturation of CB1 by endogenous cannabinoids in the explants, the DAGLα inhibitor tetrahydrolipstatin (THL) was used to inhibit endocannabinoid synthesis. THL caused a marked increase of TRH release. While WIN 55,212-2 alone had no effect on TRH release, it significantly decreased TRH release when 2-AG synthesis was blocked by THL indicating that a tonic endocannabinoid release inhibits TRH release from axons of the median eminence. Data are presented as % of control group and as mean ± SEM (N= 5). Data were analyzed by one way ANOVA and Tukey post hoc test. *= significantly different from control, *=P<0.05, **= P<0.01; #= significantly different from THL treated group (P<0.05). The amount of TRH released during 2x 10 min by the control groups was 80 ± 4 pg and residual intracellular TRH was 1860 ± 40 pg/2 ME explants. There was no difference in residual intracellular TRH between control and drug treated groups. Abbreviations: WIN=WIN55,212-2, THL=tetrahydrolipstatine.*

To determine whether glutamate or TRH released from the hypophysiotropic TRH axons may influence β2-tanycytes, the expression of the glutamate receptor subunits TRH receptors and glutamate transporters was studied in these cells (Table 1). A high level of SLC1A3 (EAAC1/EAAT3) glutamate transporter mRNA and low level of SLC1A1 (GLAST/EAAT1) and SLC1A2 (GLT-1/EAAT2)

mRNA was detected in β-tanycytes, while SLC1A6 (EAAT4) and SLC1A7 (EAAT5) glutamate transporters were not expressed.
Among the AMPA receptor subunits, mRNA of GRIA1 and GRIA2 was observed. GRIK3 was the kainite subunit with the highest expression, followed by GRIK2,4,5 that although low, was still detectable. GRIN3A was the only NMDA receptor subunit and GRM4 the only metabotropic glutamate receptor detected in β-tanycytes, but both had relatively low expression level. TRH receptors were not observed in the tanycytes.
These data suggest that glutamate effects on β2-tanycytes occur primarily *via* AMPA and kainate receptors and the glutamate transporter, SLC1A3.

Table 1. Expression of glutamate and TRH receptors and glutamate transporters in the β-tanycytes

Expression in beta tanycytes (CTgeomean $_{\text{housekeeping genes}}$ - Ctgene ± SEM)	**Short name of the gene**	**Description**
Genes expressed in tanycytes		
5.52 ± 0.92	SLC1A1	solute carrier family 1, member 1
4.50 ± 0.34	SLC1A2	solute carrier family 1, member 2
-0.15 ± 0.26	SLC1A3	solute carrier family 1, member 3
2.89 ± 0.17	GRIA1	glutamate receptor, ionotropic, AMPA1 (alpha 1)
4.37 ± 0.51	GRIA2	glutamate receptor, ionotropic, AMPA2 (alpha 2)
5.97 ± 0.68	GRIK2	glutamate receptor, ionotropic, kainate 2 (beta 2)
-0.59 ± 0.10	GRIK3	glutamate receptor, ionotropic, kainate 3
5.81 ± 0.27	GRIK4	glutamate receptor, ionotropic, kainate 4
2.57 ± 0.35	GRIK5	glutamate receptor, ionotropic, kainate 5 (gamma 2)
3.15 ± 0.09	GRIN3A	glutamate receptor ionotropic, NMDA3A
5.29 ± 0.16	GRM4	glutamate receptor, metabotropic 4
1.57 ± 0.25	DIO2	deiodinase, iodothyronine, type II
5.46 ± 0.31	DAGLA	diacylglycerol lipase, alpha
Genes do not expressed in tanycytes		
8.07 ± 0.61	SLC1A6	solute carrier family 1, member 6
UD	SLC1A7	solute carrier family 1, member 7
6.83 ± 1.68	GRIA3	glutamate receptor, ionotropic, AMPA3 (alpha 3)
6.85 ± 0.58	GRIA4	glutamate receptor, ionotropic, AMPA4 (alpha 4)
10.24 ± 0.33	GRIK1	glutamate receptor, ionotropic, kainate 1
6.80 ± 0.75	GRIN1	glutamate receptor, ionotropic, NMDA1 (zeta 1)
6.88 ± 0.30	GRIN2A	glutamate receptor, ionotropic, NMDA2A (epsilon 1)
6.54 ± 0.21	GRIN2B	glutamate receptor, ionotropic, NMDA2B (epsilon 2)
UD	GRIN2C	glutamate receptor, ionotropic, NMDA2C (epsilon 3)
8.26 ± 0.62	GRIN2D	glutamate receptor, ionotropic, NMDA2D (epsilon 4)
UD	GRIN3B	glutamate receptor, ionotropic, NMDA3B
11.77 ± 1.98	GRM1	glutamate receptor, metabotropic 1
UD	GRM2	glutamate receptor, metabotropic 2
6.88 ± 1.21	GRM3	glutamate receptor, metabotropic 3
6.38 ± 0.73	GRM5	glutamate receptor, metabotropic 5
UD	GRM6	glutamate receptor, metabotropic 6

9.20 ± 0.27	GRM7	glutamate receptor, metabotropic 7
UD	GRM8	glutamate receptor, metabotropic 8
8.08 ± 0.41	TRHR1	thyrotropin-releasing hormone receptor 1
6.86 ± 1.59	TRHR2	thyrotropin-releasing hormone receptor 2

Genes were considered to be expressed in β-tanycytes if the ΔCT value was lower than the ΔCT of GRM5.

To elucidate the effect of glutamate and TRH on the β2-tanycytes, patch clamp electrophysiology was performed. The membrane potential of the β2-tanycytes was -77.52±0.47 mV (n=83) under control conditions. Four different glutamate concentrations were applied to the cells, each causing dose-dependent depolarization of β2-tanycytes (glutamate treatments induced change of membrane potential: control: 0.25±0.42 mV, n=6; 250 µM: 4.29±0.46 mV, n=11, P=0.038; 500 µM: 7.53±0.99 mV, n=12, P<0.001; 750 µM: 8.59±0.94 mV, n=8, P<0.001 and 1000 µM:
6.85±0.83 mV, n=6, P<0.001; Fig. 3A). Treatment with 250 µM glutamate caused a significant depolarization, but significantly less than the treatment with of 500 µM glutamate (P=0.049). As 500 µM had similar effect to 750 µM and 1000 µM concentrations, 500 µM was selected for further studies.

To exclude the possibility that the effect of glutamate was mediated by TTX insensitive release of transmitters from non-tanycyte cell types of the ME, an outside-out patch clamp experiment was performed. Glutamate treatment caused large inward currents (-181.29±28.43 pA, n=4, P<0.01) (Fig. 3B) even when the tanycyte cell body was displaced into the third ventricle. The effect of glutamate disappeared during the washout period, indicating that the observed effect of glutamate was exerted directly on the β2-tanycytes. TRH had no effect on the membrane potential of tanycytes.

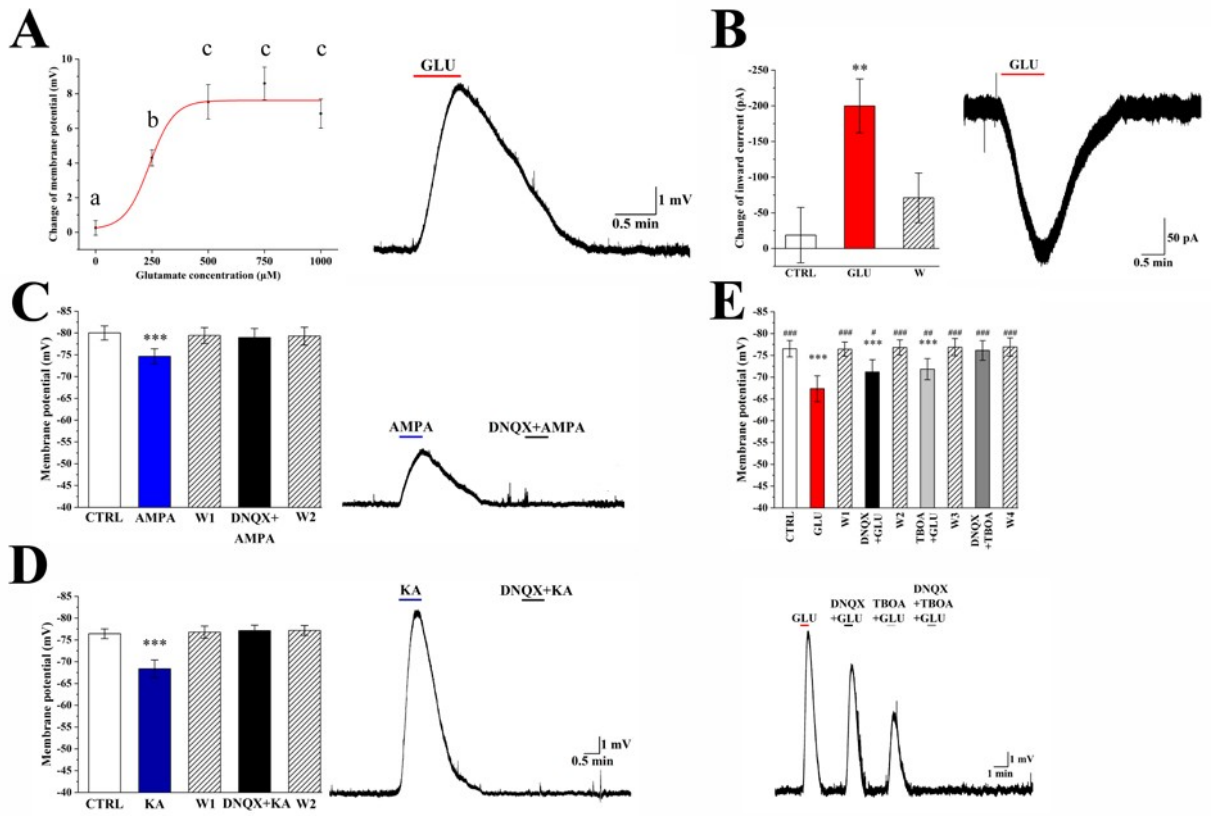

Figure 3. *Glutamate depolarizes the β2-tanycytes via activation of AMPA and kainite receptors and via glutamate transport. Representative traces illustrate the effects of pharmacological treatments on the β2 tanycytes.*

(A) Glutamate induced a dose dependent depolarization of β2-tanycytes. A representative trace illustrates the change of the membrane potential of a β2-tanycyte in response to 500 µM glutamate. (B) Glutamate (500 µM) evoked a large inward current on β2-tanycyte outside-out

*preparations, demonstrating that glutamate directly influences the tanycytes. Similar to glutamate, both (C) AMPA and (D) kainate depolarized the β2-tanycytes, and the effects prevented by the administration of the AMPA and Kainate receptor antagonist, DNQX (500 μM). (E) While DNQX and TBOA caused significant, but only partial reduction of the glutamate induced depolarization, the combination of the two inhibitors completely blocked the effect of glutamate, indicating that the effect of glutamate on the membrane potential of β2-tanycytes is mediated via AMPA and kainate receptors and by TBOA-sensitive glutamate transport. Data are expressed as mean ± SEM and were analysed with repeated measure ANOVA followed by Bonferroni post hoc test. Data with different letters on (A) are significantly different (P<0.05). * = significantly different from control, # = significantly different from glutamate treatment. * and # = P< 0.05; ** and ## P<0.01; *** and ### = P<0.001. Abbreviations: CTRL=control, GLU=glutamate, KA=kainate,W=washout.*

To investigate the receptor types that mediate glutamate-induced depolarization of β2-tanycytes, the effects of glutamate receptor agonists were studied. Similar to glutamate, both AMPA (100μM; 5.37±1.09 mV; n=8, P<0.001; Fig. 3C) and kainate (125 μM; 8.04±2.08 mV, n=7, P<0.001; Fig. 3D) markedly depolarized the β-tanycytes. Bath application of the AMPA and kainate receptor antagonist, DNQX (500 μM), prevented these effects (Fig. 3C, D).

In contrast to AMPA and kainate, NMDA had no effect on the membrane potential of tanycytes, even at high concentration (0.5 mM: 1.41±0.65 mV, n=3, P=0.42 and 4 mM: 2.12±0.3 mV, n=3, P=1.00.).

To determine whether the effect of glutamate on the membrane potential of β2-tanycytes is mediated exclusively *via* AMPA and kainate receptors, hypothalamic slices were treated with glutamate in the presence of DNQX. Inhibition of the kainate and AMPA receptors caused a significant, but only partial inhibition of the β2-tanycytes (glutamate: 9.18±1.55 mV, n=9, P<0.001 vs. control; glutamate+DNQX: 5.23±1.24 mV, P<0.001 vs. control and P=0.019 vs. glutamate; Fig. 3F**)**. Therefore, we determined whether glutamate transport also contributes to glutamate-induced depolarization. Similar to DNQX, the glutamate transporter inhibitor TBOA caused a partial inhibition of the glutamate-induced depolarization (glutamate+TBOA: 4.68±0.91 mV, n=9, P=0.001 vs. control and P=0.002 vs. glutamate; Fig. 3F). However, the combination of DNQX and TBOA completely blocked the effect of glutamate (0.40±0.61 mV, n=9, P=1.00 vs. control and P<0.001 vs. glutamate; Fig. 3F), demonstrating that glutamate depolarizes the tanycytes *via* a combination of AMPA and kainate receptor mediated effects and glutamate transport.

Optogenetic activation of the axon terminals of the TRH neurons around the end feet processes of β2-tanycytes in the external zone of the median eminence consequently caused a 0.75 ± 0.14 mV (P<0.001) depolarization of the patched β2-tanycyte cell bodies in the ventricular wall of the ME (Fig. 4). The peak of the depolarization was reached 51.74 ± 2.93 ms after the start of the optogenetic activation, the velocity of this depolarization was 0.016 ± 0.005 mV/ms. Examination of the first derivative (dV/dt) of the membrane potential showed two peaks suggesting, that the repolarization has two phases (Fig. 4C). The fast depolarization was followed by a fast -0.29 ± 0.09 mV repolarization with 126.66±10.73 decay time and then by a very slow repolarization (decay time: 3127.60 ± 446.29 ms). This suggested that the TRH axons may influence tanycytes by the release of at least two different compounds: a fast acting transmitter and a transmitter with long lasting effect. Simultaneous administration of DNQX and TBOA markedly decreased the optogenetic activation induced depolarization of tanycytes (0.32±0.08 mV; P<0.01; Fig. 4). The velocity of this depolarization was significantly lower than the velocity of depolarization induced by glutamate alone (0.004 ± 0.002; P<0.05; Fig. 4E). The first derivative (dV/dt) of the membrane potential had only one peak (Fig. 4C) in the presence of antagonists, indicating that this effect has only one phase. The two antagonists prevented the first fast phase. These data demonstrate that the TRH axons influence the tanycytes with a fast acting transmitter, glutamate, and also by a currently unknown transmitter(s) with longer lasting effect.

Optic stimulation of slices from TRH-IRES-tdTomto mice where the TRH axons expressed tdTomato (but did not express channelrhodopsin) had no effect on the membrane potential of tanycytes (Fig 4B).

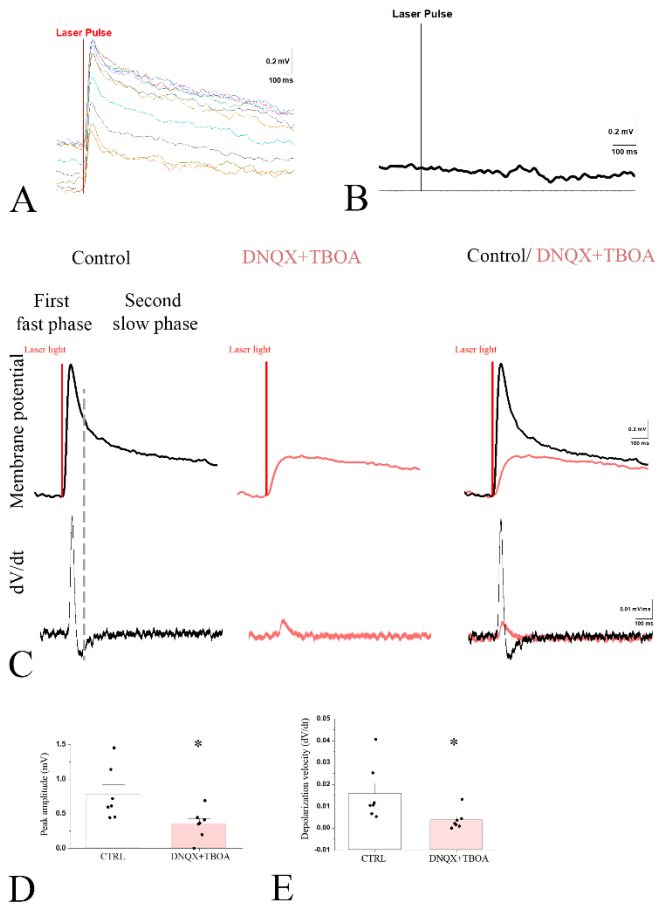

Figure 4. *The optogenetic activation of TRH axons in the ME induces depolarization of β2-tanyctes which effect is partially mediated by glutamate. The membrane potential changes of a representative tanycyte in response to 10 consecutive optic activation of TRH axons (A). The membrane potential of tanycytes is not influenced by the light impulse if the TRH axons do not express channelrhodopsin (B). (C) illustrates the mean response of the tanycyte membrane potential in response to 10 sweeps of optic stimulation of TRH axons. The upper traces show the membrane potential changes of the tanycyte under control conditions (black line), when the same cell was treated with a combination of DNQX (0.5µM) and TBOA (1mM) (red) and the overlay of the two traces. The lower graphs illustrate the first derivative (dV/dt) of the membrane potential changes. The two peaks of the dV/dt of the control trace suggest that the optic stimulation induced membrane potantial change has two phases under control conditions: an initial fast phase including a fast depolarization and a fast repolarization followed by a long lasting phase of slow repolarization. When inhibitors are applied, the membrane potential change has only a single phase and markedly decreased amplitude. The overlay of the two traces indicates that the speed of depolarization is markedly decreased in the presence of DNQX and TBOA. Bar graphs summarize the effects of activation of TRH axons on the peak amplitude of membrane potential (D) and the depolarization velocity under control condition and when the cells are treated with DNQX+TBOA. Data are expressed as mean ± SEM and were analysed with paired Student's t test. * = significantly different (P<0.05).*

As increase of intracellular Ca^{2+} levels is a crucial signal to increase DAGlα activity, the effect of glutamate was studied on the intracellular Ca^{2+} level of β2-tanycytes. Glutamate treatment (500 µM) caused a robust increase of fluorescent intensity values (FIV) of β2-tanycytes (baseline: 189.19 ± 26.52 treatment: 416.13 ± 31.28; $P < 0.001$; $N_{cell} = 56$) increasing it to 219.95 ± 27.66% of the baseline values (Fig. 5). To determine whether similar to the effect of glutamate on the membrane potential of tanycytes, the effect of glutamate on the intracellular Ca^{2+} level can also be blocked by inhibition of AMPA and kainite receptors and glutamate transport, we administered DNQX (0.5 mM) and TBOA (1 mM) during the glutamate treatment. Application of these inhibitors completely prevented the increase of FIV (baseline: 242.13±28.06 treatment: 250.27±28.67; Ncell = 79; P=0.99) (Fig. 5).

To test whether the main transmitter of the hypophysiotropic TRH neurons can influence the intracellular Ca^{2+} level of β2 tanycytes, the effects of TRH and its combination with glutamate were tested (Fig. 5). TRH treatment (5 µM) caused no significant changes neither in the FIV of β2-tanycytes (control: 187.46 ± 30.58 treatment: 186.71 ± 30.42) nor the percentage values of FIV (99.79 ± 0.30%) when compared to the control, baseline values (P=0.9; $N_{cell} = 34$).

Treatment of β2-tanycytes with the combination of TRH + Glutamate (5 and 500 µM,

respectively) caused a robust increase of FIV (control: 154.70±26.09, treatment: 323.85 ± 34.68) increasing it to 209.34±16.88% of the baseline values (P = 0.002; N_{cell} = 37). The effect of combined TRH+glutamate treatment, however, did not differ from the effect of treatment with glutamate alone (P=0.99).

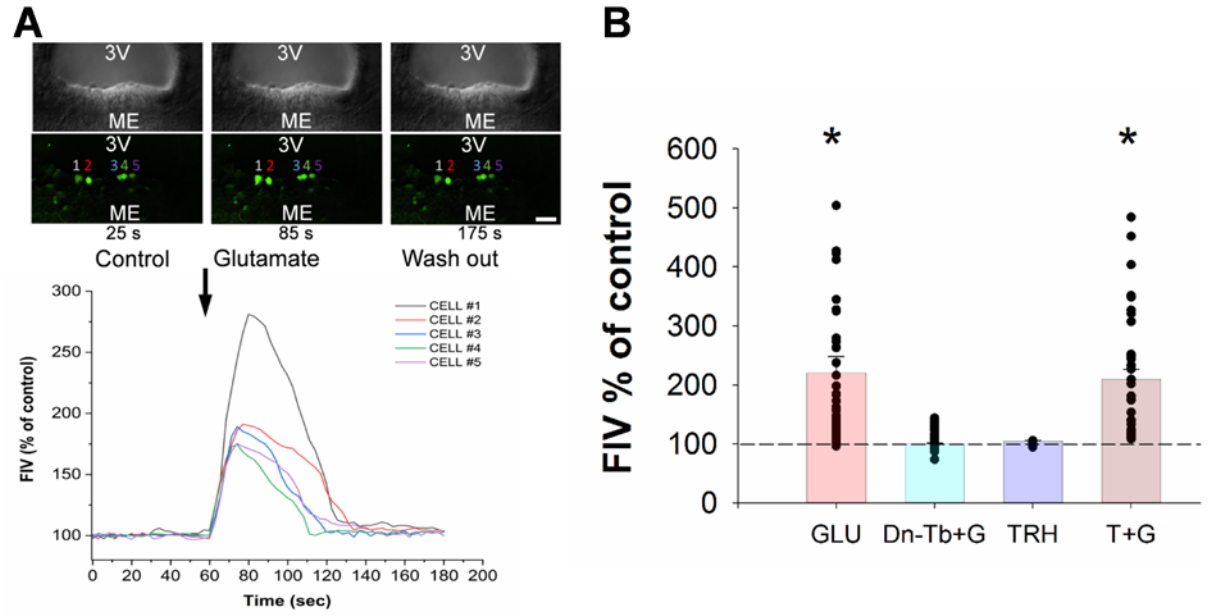

Figure 5. *Effects of glutamate and TRH treatment on the intracellular Ca^{2+} level of β2-tanycytes. The changes of fluorescent intensity values (FIV) of the Ca^{2+} sensitive dye Fluo-4 AM was measured as a marker of the changes of intracellular Ca^{2+} level of β2-tanycytes after different treatments in vitro. (A) Representative recording shows that glutamate treatment (500 μM) increases FIVs in the measured β2-tanycyte perikarya. Black arrow represents the beginning of the glutamate treatment. (B) Bar graph summarizes effects of different treatments. GLU = glutamate (500 μM, N=56); Dn-Tb+G=DNQX+TBOA + GLU (DNQX+TBOA, 0.5 mM and 1 mM respectively; N=79) TRH (5 μM, N=34); T+G = TRH+glutamate (5 and 500 μM, respectively; N=37). Only glutamate and TRH+glutamate treatment increased FIV% values significantly (P<0.001 and P = 0.002, respectively). TRH alone could not initiate any significant changes. The effects of Glutamate alone and the combined Glutamate+TRH treatment did not differ from each other (P=0.999). Treatment of sections with DNQX+TBOA prevented the increase of intracellular Ca^{2+} level induced by glutamate treatment (DNQX+TBOA+GLU vs. control: P=0.999). Data are shown as mean ± SEM, for statistical comparison One Way ANOVA (F (4, 235)) = 15.849; P < 0.0001) was used followed by Bonferroni post hoc test. * = significantly different from control P < 0.05.*

To determine whether endogenous glutamate can stimulate the 2-AG synthesis of tanycytes, the effect of glutamate receptor and transporter inhibitors was studied on the 2-AG content of ME explants. The 2-AG content of control ME explants was readily detected (0.54±0.08 ng/mg tissue). Simultaneous inhibition of AMPA and kainate receptors and the TBOA sensitive glutamate transporters caused an approximately 50% decrease of the 2-AG content of the ME explants (0.29±0.03 ng/mg tissue; P=0.01) suggesting that endogenous glutamate stimulates 2-AG synthesis in tanycytes.

In summary, these data demonstrate that a regulatory microcircuit exists between β-tanycytes and hypophysiotropic TRH axons, utilizing the release of endocannabinoids and glutamate. This circuit may contribute to controlling the release of TRH into the ME and may be an important mechanism to synchronize of the activity of hypophysiotropic terminals. The manuscript describing these data is was accepted in the iScience.

3) Other results

We have shown that tanycytes express PACAP receptor and PACAP stimulates the D2 expression in the tanycytes that is accompanied by inhibition of the TRH gene expression in the PVN. (Endocrinology 157(6):2356-66, 2016)

We aimed to determine the onset of thyroid hormone-mediated hypothalamic-negative feedback and studied how local hypothalamic metabolism of thyroid hormones could contribute to this process in developing chicken. In situ hybridization revealed that whereas exogenous T_4 did not induce a statistically significant inhibition of TRH expression in the paraventricular nucleus at embryonic day (E)19, T_4 treatment was effective at 2 days after hatching (P2). In contrast, TRH expression responded to T_3 treatment in both age groups. TSHβ mRNA expression in the pituitary responded to T_4 in a similar age-dependent manner. Type 2 deiodinase (D2) was expressed from E13 in tanycytes of the mediobasal hypothalamus, and its activity increased between E15 and P2 both in the mediobasal hypothalamus and in tanycyte-lacking hypothalamic regions. Nkx2.1 was coexpressed with D2 in E13 and P2 tanycytes and transcription of the *cdio2* gene responded to Nkx2.1 in U87 glioma cells, indicating its potential role in the developmental regulation of D2 activity. The T_3-degrading D3 enzyme was also detected in tanycytes, but its level was not markedly changed before and after the period of negative feedback acquisition. These findings suggest that increasing the D2-mediated T_3 generation during E18-P2 could provide the sufficient local T_3 concentration required for the onset of T_3-dependent negative feedback in the developing chicken hypothalamus. (Endocrinology 157(3):1211–1221, 2016)

To determine whether tanycytes communicate with each other via Connexin 43 (Cx43) gap junctions, individual tanycytes were loaded with Lucifer yellow (LY) through a patch pipette. In all cases, LY filled a larger group of tanycytes as well as blood vessels adjacent to tanycyte processes. The Cx43-blocker, carbenoxolone, inhibited spreading of LY. The greatest density of Cx43-immunoreactive spots was observed in the cell membrane of α-tanycyte cell bodies. Cx43-immunoreactivity was also present in the membrane of β-tanycyte cell bodies, but in lower density. Processes of both types of tanycytes also contained Cx43-immunoreactivity. At the ultrastructural level, Cx43-immunoreactivity was present in the cell membrane of all types of tanycytes including their ventricular surface, but gap junctions were more frequent among α-tanycytes. Cx43-immunoreactivity was also observed in the cell membrane between contacting tanycyte endfeet processes, and between tanycyte endfeet process and axon varicosities in the external zone of the median eminence and capillaries in the arcuate nucleus and median eminence. These results suggest that gap junctions are present not only among tanycytes, but also between tanycytes and the axons of hypophysiotropic neurons. Cx43 hemichannels may also facilitate the transport between tanycytes and extracellular fluids, including the cerebrospinal fluid, extracellular space of the median eminence and bloodstream. (Brain Res. 2017 Oct 15;1673:64-71.)

Thyroid hormone (TH) is present in the systemic circulation and thus should affect all cells similarly in the body. However, tissues have a complex machinery that allows tissue-specific optimization of local TH action that calls for the assessment of TH action in a tissue-specific manner. To study tissue-specific TH action, we generated a TH action indicator (THAI) mouse model. The model uses a firefly luciferase reporter readout in the context of an intact transcriptional apparatus and all elements of TH metabolism and transport and signaling. The THAI mouse allows the assessment of the changes of TH signaling in tissue samples or in live animals using bioluminescence, both in hypothyroidism and hyperthyroidism. Beyond pharmacologically manipulated TH levels, the THAI mouse is sufficiently sensitive to detect

deiodinase-mediated changes of TH action in the interscapular brown adipose tissue (BAT) that preserves thermal homeostasis during cold stress. The model revealed that in contrast to the cold-induced changes of TH action in the BAT, the TH action in this tissue, at room temperature, is independent of noradrenergic signaling. Our data demonstrate that the THAI mouse can also be used to test TH receptor isoform-specific TH action. Thus, THAI mouse constitutes a unique model to study tissue-specific TH action within a physiological/pathophysiological context and test the performance of thyromimetics. In conclusion, THAI mouse provides an in vivo model to assess a high degree of tissue specificity of TH signaling, allowing alteration of tissue function in health and disease, independently of changes in circulating levels of TH. (Endocrinology. 2018 Feb 1;159(2):1159-1171). We have patented this mouse model. The patent from Hungary and EU were granted, while patenting in the USA is ongoing.